Rev. Mexicana Astron. Astrof., **18**, 125-143 (1989)

PROPERTIES OF STAR CLUSTERS IN THE LARGE MAGELLANIC CLOUDS

Cesare Chiosi

Department of Astronomy
University of Padova, Italy

RESUMEN. Discutimos las propiedades principales de familias de cúmulos estelares en la Nube Mayor de Magallanes (NMM). Revisamos los modelos de estrellas de masa pequeña e intermedia con la presencia de excesos convectivos y describimos un algoritmo para el tratamiento de la fotometría de los cúmulos: diagramas de color magnitud, funciones de luminosidad (FL), magnitudes, colores integrados y masas totales. Presentamos fotometría CCD en *BV* de Johnson de NGC 1866 y la empleamos para probar los modelos de estrellas de masa intermedia con excesos convectivos. Encontramos que estos modelos explican el diagrama C–M y la FL mejor que otros. También comparamos los datos NGC 1831. Discutimos el problema de los sistema binarios para explicar la discrepancia en la determinación de las edades de los cúmulos por medio de las estrellas de la secuencia principal y de las gigantes rojas. Discutimos la formación estelar retrasada en NGC 1831. Analizamos las calibraciones teóricas entre los colores integrados y las edades como función de la composición química para interpretar la causa física de su distribución bimodal en (*B–V*). Encontramos que ésta se debe simplemente al tipo de distribución de edades de los cúmulos. Presentamos nuevas determinaciones de masas totales de cúmulos. Comentamos sobre la historia de la formación estelar de las estrellas de campo en la NMM.

ABSTRACT. We discuss in this paper, the main properties of the family of star clusters in the large Magellanic Cloud (LMC). To this aim, we first review the stellar models for low and intermediate mass stars in occurrence of convective overshoot, and then describe an algorithm suitable for a theoretical approach to cluster photometry (colour magnitude C–M) diagrams, luminosity functions (LF), integrated magnitudes and colours, and total masses). The Johnson *B–V* CCD photometry of the stellar content of NGC 1866 is presented and used to test the theoretical models for intermediate mass stars with convective overshoot. The conclusion of this analysis is that these models fit the C–M diagram and LF of NGC 1866 much better than any other type of models in the literature. In addition to this, the Johnson *B–V* CCD photometry of NGC 1831, another populous cluster of LMC, is presented and analyzed by means of the same stellar models. In particular, we discuss the effect of unresolved binary stars on alleviating the discrepancy between the age determined from the main sequence stars and the age determined from the red giant stars. Following an idea advanced by Eggen and Iben (1988, 1989) to explain the existence of blue stragglers in young disk aggregates, we explore the possibility that delayed star formation has taken place in NGC 1831. The final part of the review deals with the integrated photometry of star clusters. Theoretical calibrations between integrated colours and age as a function of the chemical composition, are briefly discussed. The aim is to derive the age distribution function of LMC cluster and interpret the physical cause of their bimodal distribution in (*B–V*). The main result is that bimodality simply originates from the kind of age distribution that LMC clusters happen to possess, whereas all other explanations put forward in literature play a marginal role. We also present new estimates of the total mass of many clusters derived from their integrated *B–V* magnitudes. Finally a few words are addressed to the issue of the history of star formation in the field stars of LMC.

Key words: **CLUSTERS GALAXIES–MAGELLANIC CLOUDS — LUMINOSITY FUNCTIONS — STARS–EVOLUTION — STARS–HERTZPRUNG–RUSSELL DIAGRAM**

1. Introduction

In this paper we report on a series of studies aimed at interpreting in a coherent fashion the properties of star clusters in LMC. To this purpose, on one hand we have undertaken an observational program to determine the Johnson BVRI CCD photometry for a large sample of clusters spanning the whole range of ages and chemical composition, on the other hand we have calculated many evolutionary tracks in the mass range 0.6 to 9 $M_{\odot}$ and with different chemical compositions, which have been followed from the main sequence till the latest evolutionary phases. The observational material is used to derive for each cluster the C-M diagram, the luminosity functions, the surface brigthness photometry, and the integrated magnitudes and colours. The theoretical models provide an homogeneous background from which the above observational properties can be derived as a function of the age, chemical composition, initial mass function, etc. The paper is organized in three parts. In the first one, the main properties of stellar models are outlined and our theoretical approch to cluster photometry is described. The second part deals with the stellar contents of two clusters, namely NGC 1866 and NGC 1831. NGC 1866 is taken as a template cluster against which stellar models can be compared and their reliability can be tested. The analysis of NGC 1866 indicates that stellar models with convective overshhot ought to be preferred, whereas the study on NGC 1831 brings into evidence the important role played by unresolved binary stars, and also suggests the possibility that star formation has occurred either on a relatively long time scale or in a series of episodes, not excluding however the possibilty that the cluster itself might be the result of merging of smaller subunits. In the third part, we address the issue of the integrated photometry (magnidutes and colours) and of their dependence on age and chemical composition. New calibrating relationships are are presented, which in principle enable us to estimate the age of a cluster from its integrated colours. We also discuss the nature of the bimodal distribution in (B-V) exhibited by LMC clusters, pointing out that the age distribution function (the final result of the cluster formation and disruption histories) is the main parameter determing the observed (B-V) colour distribution. In addition to this, we present preliminary results of a study aimed at deriving the total mass of any cluster from its integrated magnitude. Finally, we briefly report on a study on the law of star formation underlying the C-M diagrams and luminosity function of stellar fields in LMC. In principle, if we are able to determine the efficiency of star (and likely cluster) formation in LMC, subtracting it from the age distribution, we may be also able to infer something on the efficiency of cluster disruption by various dynamical processes all over the galaxian lifetime.

2. Review of Stellar Evolution with Convective Overshoot

In the classical view of stellar evolution, semiconvection caused by the high radiation pressure and electron scattering opacity affects the mass extention of convective cores of massive stars, during both core H and He-burning phase, whereas a similar phenomenon, driven by the opacity difference between carbon-rich and carbon poor-mixtures affects those of intermediate and low mass stars, however limited to the core He-burning phase. These topics have been the subject of many theoretical studies (see the review articles by Chiosi 1986) and are still a matter of a vivid debate. However, in addition to the problem of semiconvection, there is a more fundamental question concerning the mass extension of convective cores, i.e. the amount of convective overshoot from their borders. This, in fact, is always expected to occur at the boundary of a convective core, where the kinetic energy of convective elements carries them a finite distance into layers which are formally stable against convection. Though simply motivated from the standpoint of physical arguments, great controversy exists on the exact amount of convective overshoot. According to the theoretical formulations of this phenomenon proposed by different authors, the overshoot distance at the edge of the formally convective core goes from zero to about 2 pressure scale heights (see Chiosi 1986 for a review of the subject and exhaustive referencing). In any case, convective overshoot gives rise in stellar models to differences in structure and evolution that are much more substantial than those given by semiconvection. In addition to the above arguments of mere theoretical nature, there are many observational facts requiring a deep revision of the basic physics, such as convective cores significantly bigger than usually assumed (see the discussion by Bertelli et al. 1985, 1986a,b; Bressan et al 1986; Maeder and Meynet 1988).

2.1 Stellar Models with Convective Overshoot

Among the possible formulations of convective overshoot, we adopt the method developed by Bressan et al. (1981), which stands on a non local view of convection, uses the mixing length theory, and takes the mean free path of convective elements as a parameter to be fixed by

comparing model results with the observational properties of star clusters. The mean free path is given by $l = \lambda Hp$, where Hp is the local pressure scale height and λ is a free parameter. The evolutionary models we are going to describe are for $\lambda = 1$, which has been found to give the most interesting results (Bertelli et al. 1985: 1986a,b; Bressan et al. 1986).

i) The Core H-Burning Phase

Stars whose initial mass is high enough to develop a convective core on the main sequence ($M > 1.1\ M_\odot$), are strongly affected by convective overshoot. In fact, owing to their more massive convective cores, they run at higher luminosities and live longer than classical models. They also extend the main sequence band over a wider range of effective temperatures, this trend increasing with the stellar mass. Massive stars ($M > 40\ M_\odot$) would spread all across the colour-magnitude (CM) diagram, were it not for the contrasting effect of mass loss (see Chiosi and Maeder 1986).

ii) The Core He-Burning Phase in Massive and Intermediate Mass Stars

The overluminosity caused by overshoot during the core H-burning phase still remains during the shell H- and core He-burning phases. The mass of the H-exhausted core, M_{He}, and the mass of the C-O rich, He-burning convective core, are increased by overshoot. However, as a consequence of the higher luminosity, the lifetime of the He-burning phase (t_{He}) gets shorter in spite of the increase in the core mass. This, combined with the longer H-burning lifetime, t_H, makes the ratio t_{He}/t_H fairly low (from 0.12 to 0.06 when the stellar mass varies from 1.6 to 9 $M_\odot$). The location of the core He-burning models in the CM diagram can be schematically summarized as follows. In massive stars, where mass loss all over the stellar life dominates, the He-burning phase takes place entirely in the blue for $M > 60\ M_\odot$, partly in the blue and partly in the red for stars in the range 60 to 20 $M_\odot$ or thereabouts, the lifetime of the two sub-phases being controlled by the mass loss rate. The blue loops of intermediate mass stars ($M < M_{HeF}$) are much less extended, whereas their dependence on chemical composition and nuclear reaction rates is the same as in classical models. This implies that the blue band of core He-burning models is less inclined in the HR diagram and, therefore, for a given chemical composition the intersection with the instability strip occurs at different luminosities, hence masses.

iii) The Core He-Burning Phase of Low Mass Stars

HB stars while burning helium in the centre, possess a convective core whose mass extension may be affected by convective overshoot. Models of HB stars have been calculated according to the Bressan et al. (1981) algorithm with $\lambda = 1$, core mass equal to 0.475 $M_\odot$ and total mass in the range 0.6 to 1.4 $M_\odot$ (Bressan et al. 1986). The most important result of these calculations is that in presence of convective overshoot, semiconvection and/or breathing pulses of convection (see Castellani et al. 1985 for details) never develop. In particular, these models predict lifetime ratios in RGB, HB and AGB that are in closer agreement with the observational ones derived from star counts in globular clusters (see Buonanno et al. 1985, for a discussion of this topic). A detailed description of these models and a comparison with the observational data for globular clusters are given in Bressan et al. (1986) to whom we refer.

iv) The Critical Masses M_{mas}, M_{up} and M_{HeF}

By virtue of the larger masses of the He and C-O core left over at the end of core H and He-burning phases respectively, the relationships between the initial mass and the mass of the He and C-O core, which define the critical masses in question are different in models with convective overshoot. The most important result is that now both M_{up} and M_{HeF} are significantly lower than in classical models. They turn out to be about 1.5 smaller than in classical models. This means that no AGB and no prolonged RGB phases are expected for stars of initial mass above the new M_{up} and M_{HeF}, respectively. The impact of this result on the observational front is straightforward and of a paramount importance.

v) The AGB Phase

Over the past few years, the evolution of AGB stars has been the subject of a great deal of theoretical studies recently reviewed by Lattanzio (1988a) aimed at understanding why carbon stars can be formed at lower luminosities than predicted by the classical models of Iben (1975a,b, 1976; Becker 1981; Becker and Iben 1979). Since the evolution along the thermally pulsing AGB phase is essentially governed by the linear relationship between the H-exhausted core mass, or equivalently the C-O core mass, and the luminosity (see Iben and Renzini 1983 for all details), this is equivalent to say that the third dredge up must operate at lower core masses than suggested by the current theory. The series of recent models by Lattanzio (1986, 1987a, 1987b, 1988a,b, 1989), Boothroyd and Sackmann (1988a-d) and Hollowell (1987, 1988) in

the mass range 1-3 $M_\odot$, in which revised algorithms for semiconvection and breathing convection, the use of better opacities, the inclusion of mass loss by stellar wind, and the estimate of the dependence of the C-O core mass at the first thermal pulse on the initial chemical composition and initial mass of the star, concur to succeed in producing models of carbon stars of quite low luminosity. Models incorporating convective overshoot (see Chiosi et al., 1987) have not yet been evolved into the thermally pulsing regime, however we may foresee that they should give similar results, since they share many features in common with models calculated with semiconvection and breathing convection. Among other things, since they predict that M_{up} is much lower than the classical value, this would help removing all very bright AGB stars as indicated by the observational data (very few AGB stars brighter than $M_b = -6$).

3. The Theoretical Approach to the Cluster Photometry

Starting from the models described in the previous section, a numerical code can be developed, which generates:

i) Synthetic HR diagrams, in which stars are distributed along a given isochrone according to evolutionary lifetimes and initial mass function (IMF). For the IMF we use the Salpeter (1955) law according to which the number of stars dN in the mass interval dm is given by

$$dN = \phi(M)\, dM, \qquad (1)$$

where $\phi(M) = A\, M^{-(1+x)}$. The constant A is fixed by the normalization condition

$$N_T = A \int_{M_L}^{M_U} M^{-(1+x)}\, dM\ . \qquad (2)$$

where N_T is the total number of stars in a cluster, whereas M_L and M_U are the minimum and maximum mass of stars allowed to form in each stellar generation. Star formation is supposed to take place either instantaneously or over a finite time period, which introduces an age spread among the stars present in a cluster of any age. A gaussian distribution with a width σ is assumed for the age dispersion. Finally, at any given age only stars up to a maximum mass M(t) can exist along the isochrone, which is supposed to include stars from the main sequence till the latest observable stage, namely before either the final explosion and/or the formation of a collapsed remnant, depending on the initial mass (cf. Renzini 1981, and Renzini and Buzzoni 1986 for more details). This makes the total number $N_T(t)$ of living stars in a cluster a decreasing function of the age. In practice a "Monte Carlo" technique is employed, which randomly distributes stars of fixed age and age dispersion along all possible evolutionary stages. All values of the stellar mass in the range M_L to M(t) are allowed, each of which weighed on the IMF. The procedure is repeated until the number of stars has grown to $N_T(t)$. Since under any plausible IMF, main sequence stars are by far more numerous than those in post main sequence stages and M_L is fairly small (0.1 $M_\odot$ or thereabouts), this way of proceeding is not very convenient, as an enormous number of trials would be required. On the other hand, observations of real clusters with nowadays instrumentation customarily provide data only for stars of the upper main sequence and later evolutionary stages. Even worse, in many cases only the brightest evolved stars can be seen. In the light of this, we prefer to replace condition (2) with the equivalent one that a fixed number of post main sequence stars N_{PMS} (blue and red giants and AGB's) is matched. The total number of living stars in a synthetic cluster follows from integrating relation (1) from M(t) down to M_L. In addition to this, the "Monte Carlo" technique we have adopted both for the mass and age distribution along a given isochrone has the advantage over similar simulations of stellar clusters that stochastic effects in the IMF are automatically taken into account (see also Becker and Mathews 1983). This effect may be particularly important in connection with short lived, yet very bright, evolutionary stages, like the AGB phase. We will touch upon this point later on.

iii) Integrated fluxes and colours. If the M_V, M_B and M_U magnitudes of each star of the synthetic cluster are known, the integrated magnitudes and colours immediately follow from summing up the fluxes of the component stars. The integrated flux in a given passband is expressed by

$$F_{\Delta\lambda} = \sum_i \phi(M_i)\ 10^{-0.4\, M_{\Delta\lambda}\,(M_i,t)}\ \Delta M \qquad (3)$$

where $M_{\Delta\lambda}(M_i,t)$ is the magnitude of a star of mass M_i at time t. All normalization factors entering the definition of $\phi(M)$ and F_λ are not of interest here. The integrated colours are computed with the relations (see Searle et al. 1973)

$$(B-V)_o = 2.5\ \mathrm{Log}(F_V/F_B) \quad \text{and} \quad (U-B)_o = 2.5\ \mathrm{Log}(F_B/F_U). \qquad (4)$$

Similar expressions hold good in the case of an isochrone with a continuous distribution of stars (masses), provided the summation is replaced by an integral and $M_{\Delta\lambda}(M_i,t)$ is considered as the magnitude in the pass band $\Delta\lambda$ of the particular stage along the isochrone to which a mass M_i corresponds. In this case, the normalization procedure can be greatly simplified by assuming A = 1. The integrated fluxes are therefore given apart from the normalization constant A. In both cases, the actual total magnitudes are given by

$$M^*_{\Delta\lambda} = -2.5\ \mathrm{Log}(A\ F_{\Delta\lambda}). \qquad (5)$$

v) Luminosity functions for the main sequence and the evolved stars. These turn out to be very very useful tools for discriminating among the various scenarios for the evolution of stars of any mass that have been proposed during the recent years (see section 1).

3.1 The Conversion to a Colour-Magnitude Diagram

The theoretical luminosities and effective temperatures are translated into M_V, M_B, M_U magnitudes and $(B-V)_o$, $(U-B)_o$ colours using tables of conversion, where colours and bolometric corrections are given as a function of the effective temperature (T_{eff}) and gravity (g). There are two main sets of Tables, i.e. the ones elaborated by Chiosi et al. (1988), which are based on model atmospheres calculatedby several authors (Bell and Gustafsson 1978; Buser and Kurucz 1978; Gustafsson et al. 1975) and extend to the UBV passbands, and those contained in the revised Yale isochrones (Green et al. 1987) which extends to the UBVRI passbands. Though similar, they differ in several details which may bear some importance in tht comparison with the observational data. Results will be presented for both sources.

4. Clusters of the LMC: NGC 1866 a Test for Convective Overshoot

Although stellar models calculated with semiconvection and breathing convection look similar to those calculated with convective overshoot, the two types of model deeply differ in many quantitative details. The characterizing features are the core H and He-burning lifetimes and evolutionary brightening from the main sequence up to the most advanced stages. These should immediately reflect into the morphology of CM diagrams of star clusters, namely the number of evolved to main sequence stars and associated luminosity functions. It goes without saying that the ideal laboratory where theories of stellar structure, in particular those concerning the domain of massive and intermediate mass stars, can be tested are the rich young clusters of the Magellanic Clouds. These in fact by virtue of their large number of stars allow statistically meaningful comparisons between theory and observations in samples of about coeval and chemically homogeneous objects even for the shortest lived evolutionary stages. To this purpose, Chiosi et al. (1988a,b) have taken accurate Johnson BV CCD photometry of the cluster NGC 1866 of the Large Magellanic Cloud (LMC) and compared its CM diagram and main sequence star luminosity function with the theoretical predictions based on both classical models and models with convective overshoot. The results of Chiosi's et al. (1988a,b) study are briefly summarized below.

NGC 1866 is a rich young cluster situated at about 2^o North of the LMC centre, whose total mass is estimated in the range 3.6 to 8.5 10^4 $M_\odot$ (Heckman 1976). It is classified as a type III in the Searle et al. (1980) system, with integrated apparent visual magnitude V = 9.73, and colours (B-V) = 0.25 and (U-B) = -0.04 (van den Bergh 1981) and colour excess E(B-V) = 0.07 (Persson et al. 1983). Johnson BV CCD photometry of 1517 stars in the central region of NGC 1866, and of 640 stars in a nearby field have been obtained with the RCA #5 CCD at 2.2m ESO telescope and reduced using the ESO version of DAOPHOT. To define the region of the cluster frame that suffers from the least degree of uncertainty by photometric incompleteness and contamination by field stars the following procedure is adopted. First, a composite CCD frame (cluster and field) is obtained superposing a few bright stars in common, and an iterative procedure is used to fix the cluster centre. Second, the surface brightness profile of the cluster is generated in a way similar to Meylan and Djorgovski (1987) and compared to the theoretical density profiles calculated from multi-mass, King-Michie models (Meylan 1987a,b; 1988) in the case of the Salpeter law with slope x = 2.35 and isotropical velocity dispersion.

The cluster turns out to possess a concentration c = log r_t/r_c = 1.5, a core radius r_c = 6."69 and a tidal radius r_t = 211."6. Furthermore, since the last point of the observed profile is at about r = 2.'40 to which a density contrast of about a factor of 10^3 corresponds, the radius r_W = 2.'45 is taken as the limiting radius beyond which the majority of stars are field objects. Third, the surface brightness profile is reconstructed from the photometric data (V and/or B magnitudes) of individual stars falling within circles of increasing radius centerd on the cluster centre. The simultaneous comparison of the surface brightness profile, the density profile, and the surface brightness profile reconstructed from individual stars, shows that the ring confined between 0.'52 and 0.'98 is the one suffering from the least degree of incompleteness by crowding and other causes, and it can be taken to represent the cluster population. The CM of the stars falling in this region is assumed as the reference CM to which theoretical models ought to be compared. This is shown in Fig.1. In this CM diagram, three regions of particular interest can be defined, namely: the region of the main sequence stars (MS), the region of red giant stars brigther than 17 V mag (BRGS), the region of red giant stars fainter than 17 V mag (FRGS). The total number of stars is 656, of which MS = 594, BRGS = 39 and FRGS = 23. This CM diagram is photometrically complete down to V = 19.2 mag. The field is given by the region of the composite CCD frame outside r_W, whose area happens to be nearly identical to that of the cluster ring. After correction for photometric completeness (crowding) and contamination by field stars by means of the zapping technique of Mateo and Hodge (1986), the total number of stars is 1020 made of MS = 954, BRGS = 41, FRGS = 25. The group of BRGS

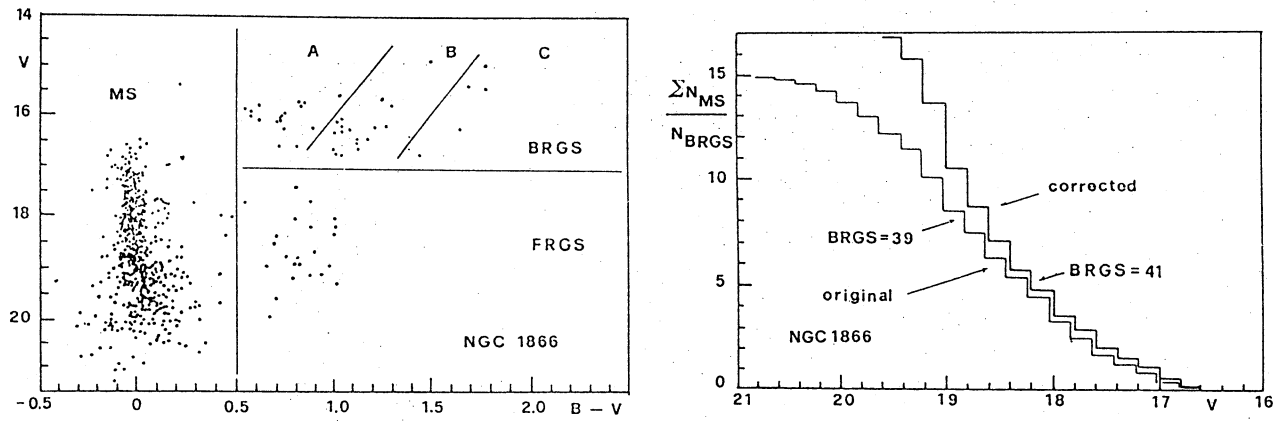

Fig.1. The CM Diagram of the selected ring of NGC 1866. Capital letters A, B and C indicate three groups of stars discussed in the text.

Fig.2. The integrated luminosity function for the main sequence stars normalized to the number of bright red giant stars (V < 17 mag) likely representing the evolved counterpart of the main sequence population (see text for more details).

likely represents the population of evolved stars belonging to the cluster, i.e. genetically linked to the populations of MS, whereas FGRS are likely field stars. NGC 1866 contains also several Cepheids: 11 well established objects (Walker 1987, and references therein) and about 10 more recent candidates (Storm et al. 1988), which are located in the middle of BRGS. The sample of BRGS can be split into three subgroups (labeled A, B and C). Group A and B contain almost equal numbers of stars and are located at the blue and red side of the instability strip, whereas group C is populated by stars (very few indeed) of the same luminosity but of much redder colour. Likely, these do not belong to the same population as those of groups A and B, but probably they are genetically related to FRGS. The luminosity function for the MS stars is presented in Fig.2. This is the integrated number of stars counted from the tip of the main sequence band down to the current magnitude bin and normalized to the number of BRGS. The

advantage of this type of luminosity function is that it can be simply related to the ratio of core H- to core He-burning lifetime. On the theoretical side, a computer code has been developed for constructing synthetic CM diagrams, luminosity functions, integrated magnitudes and colours in the UBVRI bands as a function of the age, chemical composition, initial mass function, total number of stars, given number of evolved stars corresponding to the observed BRGS, and finally stellar evolution input. This algorithm also allows for dispersion in age and fluctuations of stochastic nature in the initial mass function. The comparison between theory and observations based on several fiducial characteristics of the the CM diagram, such as the mean location of the main sequence band, its terminal luminosity, the mean luminosity of the blue and red giant stars, the tip of the blue loop (if present), and the location of the reddest stars (Hayashi limit) allows to derive the age and the chemical composition and to estimate the distance modulus in the two alternatives for the stellar evolution background, namely classical models and models with overshoot. The simultaneous fit of the above constraints indicates that the appropriate chemical composition is Y = 0.28 and Z = 0.02 (or slightly less say Z = 0.010-0.015), the true distance modulus is $(m-M)_o$ = 18.6 mag in good agreement with the value determined from the near infrared photometry of Cepheid stars (Welch et al. 1987), and the age is 200×10^6 yr for models with overshoot, or 70×10^6 yr for classical models. However, with these latter models the fit of the red giant stars is rather poor, as they turn out to be fainter than the mean luminosity of the loop and bluer than the Hayashi limit. Other combinations of age and chemical composition can be neglected as they would lead either to a very poor fit of the global properties of the CM diagram or to unacceptably low distance moduli. While the CM diagram does not clearly indicate the underlying evolutionary scheme, this is possible looking at the integrated main sequence luminosity function normalized to the number of post main sequence stars (N_{PMS}). The comparison with the observational luminosity function strongly favours models with convective overshoot. In other words, the star counts in the clusters suggest that the ratio of core H to He-burning lifetimes and the range of luminosity spanned by main sequence stars, whose masses are compatible with those of the evolved stars, must be smaller and wider, respectively, than given by the classical models. This is possible only if more efficient mixing occurs all over a star's evolutionary history and not only in stages beyond the main sequence phase. It is worth emphasizing that other mixing processes like semiconvection and/or breathing convection, would not be able to satisfy the observational demand, since they tend to increase the number of evolved stars with respect to those of the main sequence. Agreement with the classical models is marginally possible only by increasing the slope of the initial mass function above 4.

5. NGC 1831: Binary Stars or Delayed Star Formation ?

NGC 1831 is another large, luminous clusters of the LMC. It is located in the sky projected proximity of NGC 1866, at about 2^o North of the centre, in a relatively clear area out of the main body of the galaxy. This cluster, having an apparent V magnitude of 11.18 and a (B-V) colour of 0.34 (van den Berg 1981) was classified as a type V by Searle et al. (1980). Recent Johnson BV CCD photometry has been obtained by Vallenari et al. (1989) using the same instrumentation, detectors and reduction technique as for NGC 1866. Previous studies of the C-M diagram of this cluster are by Hodge (1963, 1984). In total about 1800 stars in the cluster and of 500 stars in a nearby field have been measured. Particular care is paid to estimate the errors in the data caused by uncertainties in the photometry and by crowding, and to isolate the portion of the cluster suffering from the least degree of incompleteness. The same method used for NGC 1866 has been followed. This allows us to set the concentration of the cluster at $c = \log r_t/r_c = 0.69$, $r_c = 29.''7$ and $r_t = 148.''6$, where r_c and r_t stand for core and tidal radius, respectively, and to isolate the annulus with radii $36.''7$ and $1.'32$ as the region best representing the cluster population. This sample of stars is then corrected for photometric completeness and contamination by field stars. The CM diagram for the annulus is shown in Fig.3, whereas the integrated luminosity function will be given below. The C-M diagram shows a well defined main sequence band terminating at about V = 18.4, a red giant clump centered at about half of a magnitude below the termination of the main sequence band and spanning the colour range 0.8 < (B-V) < 0.9, a sprinkle of stars of the same luminosity but of bluer colour scattered toward the main sequence band, and finally a scarce population of bright red stars. With the aid of the method developed by Da Costa et al. (1984), the metallicity of the cluster is estimated to be about [Fe/H] = -0.6 or equivalently Z = 0.004. The colour excess E_{B-V} = 0.04 is taken from Burstein and Heiles (1982), whereas the intrinsic distance modulus $(m-M)_o$ = 18.6 is assumed.

5.1 Fit of the C-M Diagram of the Cluster Stars

With the adopted true distance modulus and extinction, the termination magnitude of the main

sequence band is $M_V = -0.32$, whereas the luminosity at the bottom of the clump of red stars is $M_V = 0.28$. These two critical luminosities can be used to set a preliminary estimate of the age (Chiosi et al. 1988). It is soon evident that, independently of the adopted chemical composition and conversion relations, the age estimated from the main sequence termination magnitude is in contrast with the age derived from the clump of red stars. Looking at the simulated C-M diagrams (Yale conversions) and the colour trend of the main sequence band, and taking into account the colour excess, we notice that metallicities as low as Z = 0.001, which would imply an age of about 5×10^8 yr, can be excluded as the theoretical main sequence turns out to be much bluer and at the same time the bulk of red giants to be at least 1.5 mag brighter than the observed ones. On the other hand, metallicities as high as Z = 0.02, for which an age of about 8×10^8 yr is found, can also be excluded as, if the termination magnitude of the main sequence band and marginally the bottom luminosity of the red giants can be matched, they both turn out to be much redder than the observed ones. In the case of the metallicity Z = 0.004, the main sequence bands agree both in luminosity and colour, but the predicted red giants are about 0.5 mag brighter than the observed ones though of about the same colour. The age in this case is approximately 8×10^8 yr. Therefore, if we impose the constraint that the termination magnitude and colour trend of the main sequence are matched,

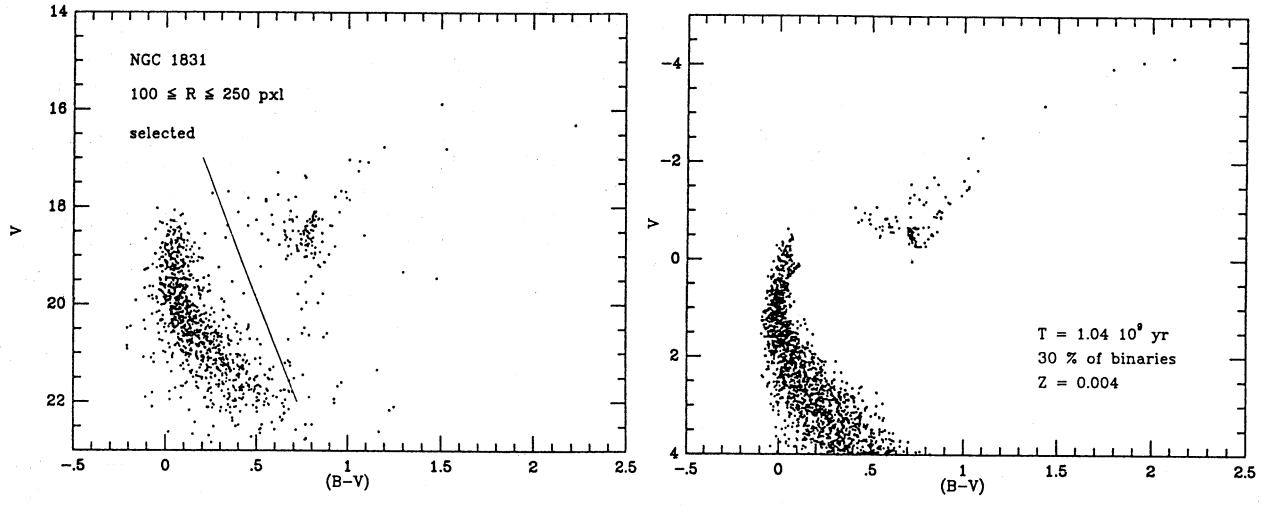

Fig.3 The reference C-M diagrams for the annulus of NGC 1831. The total number of stars is 1228, of which 1072 bluer and 146 redder than the line drawn in the C-M diagram. The magnitude V = 19 separates the bright red giants from the faint ones: $N_{BRGS} = 130$ and $N_{FRGS} = 16$.

Fig.4 Theoretical C-M diagram for the metallicity Z = 0.004, the age $T = 1.04 \times 10^9$ yr, the Salpeter law with x = 1.35, binary stars and photometrical errors. The number of $N_{PMS} = 125$. The percentage of unresolved binaries amounts to 30% and their mass ratio $Q = M_1/M_2$ is the range 0.8 to 1.25

difficulties arise in reproducing the luminosity and colour of the red giants or, conversely, in reconciling their age with that of main sequence stars. Similar results are obtained with the Chiosi et al. (1988) conversions, although different ages are derived.

There are several causes for the disagreement between the expected and observed location of red giants with respect to the termination magnitude of the main sequence band, among which we recall: i) inadequacy of the conversion relationships; ii) inadequacy of the relationships converting luminosities and effective temperatures into visual magnitudes and (B-V) colours;

iii) underestimate of the visual extinction for the red giant stars. in the sense that A_V should be much higher than simply given by $A_V = 3.1\ E_{(B-V)}$ or the colour excess assigned to the cluster should be greater than $E_{(B-V)} = 0.04$; iv) inadequacy of the theoretical models for intermediate mass stars (the turn-off mass here is about 2.5 $M_\odot$) in the sense that the luminosity of the core He-burning band is too bright with respect to the main sequence tip; v) the observational termination magnitude does not correspond to the stage of core H-exhaustion of single stars, but to a more complex situation where the occurrence of unresolved binaries of suitable mass ratio and separation extends the main sequence band to brighter magnitudes. Points (i) through (iii) are found to yield a marginal effect, whereas points (iv) and (v) may be more important. In the following we will discusss these two latter points in some detail.

Stellar Models. The stellar models in use are those with convective overshoot during the core H and He-burning phases. It has been already said that among other properties, these models are known to predict different H and He-burning lifetimes and much higher luminosities during these two phases with respect to classical models (Becker 1981; Castellani et al. 1985; Lattanzio 1986, 1989; Mazzitelli and D'Antona 1986; Chieffi and Straniero 1988). In particular, in the mass range we are interested in, the luminosity of the core He-burning phase (loop or clump) is higher than the tip luminosity of the main sequence band, whereas in classical models this difference in the luminosity of the two types of star is much less pronounced. Since this is exactly the kind of models we would need to alleviate the above discrepancy, we might be tempted to conclude that classical models should used instead of those with convective overshoot. However, the studies by Barbaro and Pigatto (1984) on red giants in clusters younger than about $2\text{-}3\times10^9$ yr, by Becker and Mathews (1983) and Chiosi et al. (1989a,b) on star counts and luminosity functions of NGC 1866, and the recent analysis of the obervational hints in favour of convective overshoot by Maeder and Meynet (1988), point out that classical models can hardly reproduce the observational data and all conclude that models with convective offer better possibilities, even though the effiency of this phenomenon is still a matter of vivid debate. Another point of controversy may reside in the opacity, and in particular its variations across different areas of the C-M diagram. The comparison with models in literature (Mazzitelli and D'Antona 1986; Castellani et al. 1985; Lattanzio 1986, 1989) is not conclusive in this respect as they are calculated with substantially different physics (seminconvection versus overshoot), whereas models of ours with convective overshoot and other opacities are not presently available. Perhaps all this is suggesting that other more subtle causes are the reason of the discrepancy in question.

Binary Stars. The occurrence of binaries among main sequence stars may not be marginal as, under suitable combination of the mass ratio, they contribute to spread the main sequence band, shift toward brighter magnitude its termination stage, and alter the luminosity function. As already reported, we can explicitly include binary stars in our synthetic C-M diagrams following the procedure proposed long ago by Maeder (1974). The effect of binary stars depends on the assumed distribution of mass ratios. If the mass ratio is close to one, a second sequence about 0.7 magnitude brighter than the sequence of single stars is generated. As the range of mass ratios is let increase, the main sequence band is scattered by at most 0.7 magnitudes at any given colour. This means, in particular, that the main sequence tip is shifted to 0.7 brighter magnitudes, and therefore the real termination magnitude fixing the age must be taken 0.7 mag below the observed one. For Z = 0.004 this corresponds to an age of 1.04×10^9 yr. The fraction of binary stars is taken to amount to 30% and the mass ratio $Q = M_1/M_2$ is assumed in the range 0.8 to 1.25. With the inclusion of the binary stars, the apparent main sequence termination magnitude is as bright as $M_V = -0.3$ in agreement with the observational determination, the red giant stars are fainter since they older than in the previoulsy fixed by the termination magnitude, and finally the red stars are scattered toward bluer colours as it occurs in the observational C-M diagram. Finally, Fig.4 shows a complete simulation of the C-M diagram of NGC 1831 in which the effects of binary stars and photometrical errors estimated by Vallenari et al. (1989) are included. This C-M diagram remarkably resembles the observational one of Fig.3. However even in this case, although the magnitude difference between the apparent tip of the main sequence and the red stars has almost entirely disappeared, the bulk giants tend to be about 0.3 mag brighter than the observed ones. More important, when binary stars are considered, the apparent tip of the main sequence can no longer be taken as a firm age indicator.

5.2 Fits of the Cluster Luminosity Function

The integrated luminosity functions for the C-M diagrams that formally match the termination magnitude of the main sequence band are shown in Fig.5, together with the observational one. These are for the age of 8×10^8 yr with no binaries and for the age of 1.04×10^9 yr and 30% of

binaries included (the C-M diagram of this latter is shown in Fig.4). Both cases have been calculated assuming N_{PMS} = 125 as indicated by star counts in the observational C-M diagram of Fig.3. The comparison with the the observational ILF, based on the assumed distance modulus and extinction, reveals that the case with age of 1.04×10^9 yr, the Salpeter law, and 30% of unresolved binaries fits the data very well. The case with the same age and percentage of binaries but flatter initial mass function (x = 0.35) would predict a similar C-M diagram but a

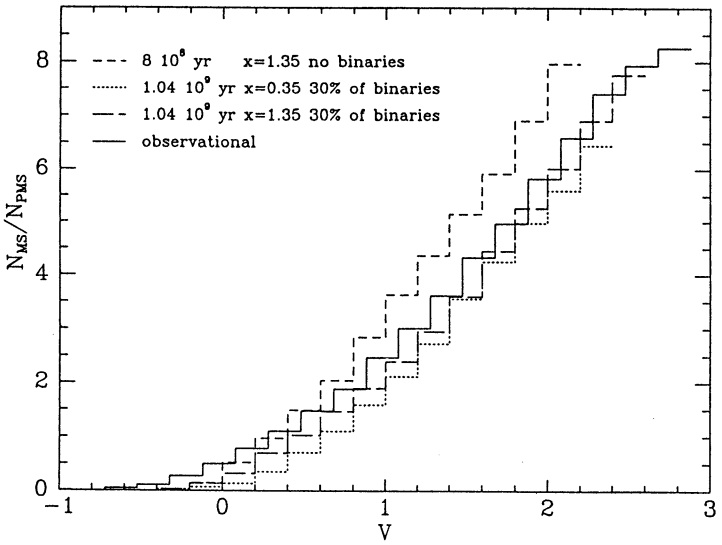

Fig.5 The integrated luminosity functions (ILF), normalized to N_{PMS} = 125, for the C-M diagrams that matched the termination magnitude of the main sequence: age 8×10^8 yr and no binaries and 1.04×10^9 yr and binaries as indicated. This latter is given for two slopes of the initial mass function, namely x = 1.35 and x = 0.35. The observational ILF is also shown. The observational ILF is normalized to N_{BRGS} = 130.

flatter ILF, which seems not to be required by the observational data. It is worth recalling that the inclusion of photometrical errors does not appreciably alter the luminosity function but only scatter the (B-V) colour.

Although we may be tempted to conclude that the age of 1.04×10^9 yr the metallicity Z = 0.004 are the appropriate parameters for the cluster, in that the termination magnitude of the main sequence and the luminosity function of these stars are reproduced, there still remains the disagreement between observed and expected location of the red giants. Considering the entity of the discrepancy in question, we may argue that suitable adjustments of the colour equation, conversion relations, extinction, and adopted stellar models (in particular the effect of higher opacities) could entirely account for the above discrepancy. However, we would like to call the attention to the broad scatter at the tip of the main sequence band (Fig.3), which cannot be reproduced by our simulations of the C-M diagram even when the effects by photometrical errors are taken into account (Fig.4). Among the many factors affecting the appearence of a star cluster's CM diagram, dispersion in age, if substantial, can easily contribute to scatter stars about the tip of the main sequence and in the region of red giants.

5.3 Prolonged Activity of Star Formation ?

Interpreting the C-M diagram of a cluster the assumption is customarily made that all stars are formed in a single episode of activity spanning a narrow age range, so that all stars are essentially coeval and an unique isochrone can be adopted to date any cluster. This basically stands on the notion that once stars with masses all over the mass spectrum are born and the first generation of supernovae (massive) has occured, all remaining gas is blown away from the cluster potential well, so that no further star formation takes place. Since the typical lifetime of a massive supernova progenitor is short (several 10^6 yr at most) the process of star formation in a cluster is considered to be sharply confined in time and, therefore, as soon as the stellar content gets older, the dispersion in the star ages to be negligible compared to the mean age of the population. However, the possibility has been suggested that star formation in stellar aggregates may take place over extended periods of time, often in recurrent bursts of activity (Eggen and Iben 1988, 1989). Exploiting further Eggen' and Iben'

(1988, 1989) suggestion, we have tried to investigate whether this idea could be applied to NGC 1831 to ameliorate the interpretation of its C-M diagram and luminosity function. To this aim we have simulated many C-M diagrams at varying law of star formation. These simulations are obtained imposing that the termination magnitude and the mean colour of the main sequence band, together with the luminositics and colours of the red giant stars are matched at a time. Furthermore, the effects of binary stars and photometrical errors are also included. We find that all of the above constraints are compatible with ages in the range $0.8\text{-}1.4\times10^9$ yr and metallicitiy Z = 0.004. Binary stars are assumed to amount to 30% of the total. and their presence is meanly meant to account for the spread of red giants toward bluer colours seen in the observational C-M diagram. As for the law of star formation, the many experiments we have performed to this purpose show that assuming it either constant or declining toward the present by a factor of two to three with respect to the initial value, yield simulations that almost perfectly match the C-M diagram and ILF of main sequence stars of NGC 1831. The C-M diagram and ILF for the case with constant star formation rate are shown in Fig.6 and Fig.7, respectively. These have been obtained imposing the same number of post main sequence stars as in the observational sample of data. We learn from our simulations that, if a prolonged activity of star formation is allowed to occur, the best fit with the observational data is obtained when the slope of the initial mass function is decreased to x = 0.35. In such a a case, the theoretical C-M diagram and ILF are both indistinguishible from the observational ones. The possibility of several bursts of activity cannot be excluded as they would lead to similar results provided they have occurred within the time interval of about 6×10^8 yr. The above simulations have been obtained assuming the same metallicity all over the period spanned by the star forming activity. Simulations (not shown here), in which various bursts of star formation, each one with a different metallicity [form Z = 0.001 (the lowest in our sets of model) to Z = 0.004], are supposed to occur, would lead to similar results. It goes without saying that these experiments are of mere exploratory nature as there is no information on inhomogeneities in the metallicity of the cluster stars.

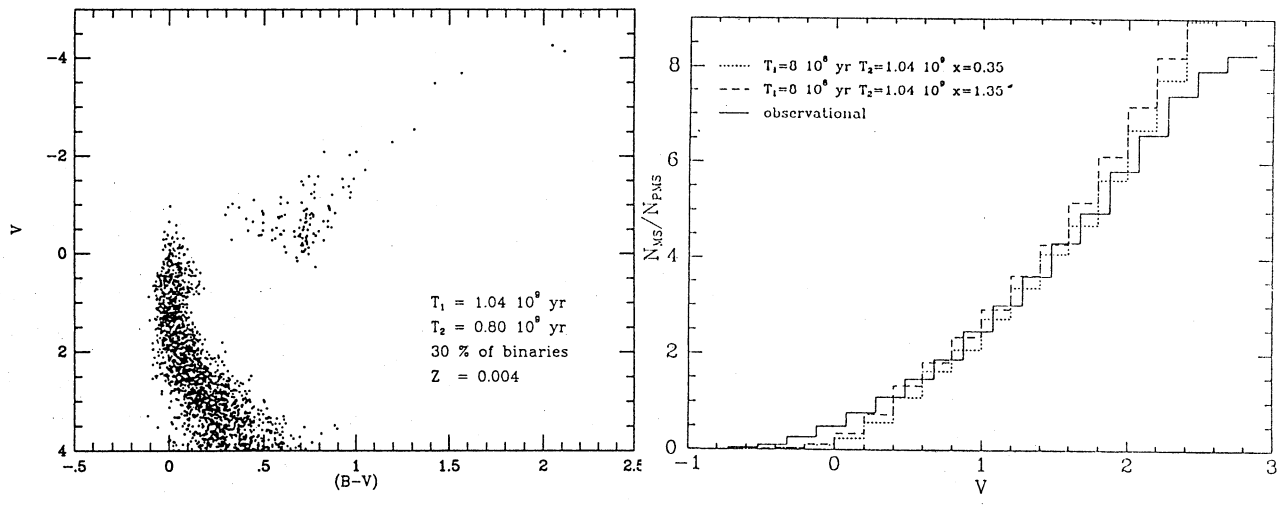

Fig.6 The C-M diagram for the simulation with a prolonged activity of star formation. The following parameters characterize this C-M diagram: metallicity Z = 0.004, N_{PMS} = 125, slope of the initial mass function x = 1.35. 30% of binaries with mass ratios $Q = M_1/M_2$ in the range 0.8 to 1.25, constant rate of star formation, and finally inclusion of photometrical errors. Tha age range covered by the stars is from T_1 to T_2 as indicated

Fig.7 The ILF for the case of constant star formation shown in Fig.6 compared to the observational one. The theoretical ILF is normalized to N_{PMS} = 125, whereas the observational ILF is normalized to N_{BRGS} = 130. We also show the ILF for the simulation with x = 0.35 (all other parameters as before), whose C-M diagram would be virtually identical to that of Fig.6

As a result of this analysis, if in NGC 1831 star formation has continued or several bursts have occured during a time scale of about 6×10^8 yr, the age of the cluster should be indicated by its oldest component, i.e. 1.4×10^9 yr. Previous episodes of star formation, if they exist, cannot be identified with the present observational data. The duration of the star forming activity we have found with our simulations does constitute an upper limit. It could in fact be shorter if the other causes of the discrepacy between main sequence and red giant stars are alleviated. Whether the agreement we have found by allowing for a prolonged activity of star formation is a mere coincidence and other explanations ought to be put forward we cannot say and, sharing Eggen's and Iben's (1988, 1989) concern, leave the subject to future studies. Nevertheless, if prolonged star formation activity is real and its time scale varies from one aggregate to another, as perhaps indicated by the results of Eggen and Iben (1989) for M67, dating clusters by means of the usual method of isochrones drawn through the data will be hard, unless realistic simulations of the cluster C-M diagram and luminosity function are used.

Concluding this section, we would like to call the attention on a point that might deserve future analysis. The observational hint toward star formation in bursts (eventually simulating a prolonged activity) within a single cluster (or aggregate) could simply reflect the possibilty that a cluster is the result of merging of smaller units. Such an idea has recently been put forward by Bathia and MacGillivray (1988), Bathia and Hatzidimitriou (1988) and Bathia et al. (1989). These authors have pointed out that taking into account the number of pairs expected from random line-up, true binary clusters can exist in LMC and that mutual merger is possible. The time scale of merging is estimated to be of the order of a few 10^7 yr to at most 10^8 yr on the basis of N-body calculations as for the instance of NGC 2214 studied by Bathia and MacGillivray (1988) for which the binary hypothesis has been advanced. Although little is known about the process of cluster formation, theoretical studies suggest that they could form in giant molecular clouds as part of complexes (Elmegreen and Elmegreen 1983) with similar ages, initial mass function and total mass of about 1×10^5 $M_\odot$, which seems to be the most common value for LMC clusters as indicated by the estimates by Alongi and Chiosi (1989) derived from the integrated cluster luminosities. This scenario for the cluster formation is perhaps also corroborated by the observational studies of Baird et al. (1974) and Elson et al. (1987, 1989) on several clusters that are suspected to belong to an unique complex. Although clusters in a pair are most likely coeval, it seems to us that an age difference of a few 10^8 yr cannot be excluded on the basis of the current understanding of this phenomenon.

6. Integrated UBVRI Colours and Magnitudes

If the integrated colours of a star cluster mainly depend on the chemical composition and age of its stellar population, then theoretical calibrations of colours as a function of the age for different compositions are very useful to obtain quantitative determinations of age and abundances of individual clusters, and thus to trace the chemical history of nearby galaxies. Over the past few years, several calibrating relationships have been derived for both Pop I and Pop II compositions. Among others, we recall Searle et al. (1973), Barbaro and Bertelli (1977), Barbaro (1981, 1982), Rabin (1982), Bruzual (1983), and Arimoto and Yoshii (1986). Even if the main properties of real clusters have already been accounted for by those calibrations, still their use is hampered by many uncertainties. First of all, they are often limited to narrow ranges of age and composition, which may generate systematic errors when different relationships are used to date clusters all over the range of possible ages. Secondly, not always all evolutionary phases implied by the types of star expected to occur in a cluster of given age are taken into account in the derivation of the integrated fluxes. In most cases, only the core H and He-burning phases are considered. Thirdly, evolutionary sequences calculated by different authors are amalgamated to derive the evolutionary scenario to start with. This also may be a source of systematic errors. Lastly, they rest on rather old evolutionary calculations, while, on the contrary, much progress has been made in this context over the recent years. In addition to this, there are properties of the star clusters that have not yet been fully understood. In particular, the clusters of LMC and SMC show two distinct groupings in the plane of integrated (B-V) colours and V magnitudes (van den Bergh 1981). In fact there are clusters either bluer than about 0.4 or redder than about 0.6 and very few in between, independently of the total V magnitude. This is also visible in the correlation between the (B-V) colour and the cluster type SWB according to the classification proposed by Searle et al (1980), where it appears that all SWB I, II and III are blue, all V, VI and VII are red, and that the blue to red transition occurs within the cluster type IV. Furthermore, the Searle et al. (1980) classification has not yet been translated into a well defined age and/or composition ranking, due to the lack of sufficient theoretical modeling of integrated

properties as a function of these two parameters. In the following we will summarize the study by Chiosi et al. (1988), in which the above topics have been analysed in a coherent fashion.

6.1 The Colour-Age Relationships

The colour- age relationships at varying chemical composition and efficiency of mass loss in the RGB and AGB phases have been calculated by Chiosi et al. (1988) to whom we refer for the discussion below. Remarkable features of the $(B-V)_o$ versus age relations are:

i) In general the $(B-V)_o$ colour gets redder at increasing age. However, under suitable combinations of the mass loss rate and chemical composition (metallicity), the colour tends to become blue again as the cluster gets older than a few billion years. This is caused by the presence in the cluster of very blue He-burning stars (mostly in HB). As expected, this effect occurs at younger ages as the mass loss rate increases.

ii) Looking at the separate contribution to $(B-V)_o$ colour from stars on the main sequence, in RGB and/or core He-burning, and later stages, we notice that in clusters of high metallicity the dominant trend is dictated by the main sequence stars with major deviations (in the sense that the colour gets much redder) at the onset of RGB and core He-burning in a red HB. In clusters of low metal content the main sequence trend, which remains also after the inclusion of core He-burning stars with mass greater than M_{HeF}, is first destroyed by the appearance of early and late AGB stars in this mass range, and then even reversed by the effect of very blue HB stars for initial masses smaller than M_{HeF}.

iii) The relative contribution of AGB stars mainly depends on the metallicity via the effect of mass loss. The rate of mass loss has been taken either from Reimers (1975) or Fusi-Pecci and Renzini (1976). In clusters of high metal content and almost independently of the particular algorithm adopted for the mass loss rate, AGB stars are expected to contribute slightly to the integrated $(B-V)_o$ colour, whereas a much greater effect is expected in clusters of low metal content.

iv) No sudden reddening in the $(B-V)_o$ colour is found at the particular ages at which the RGB and AGB phases develop for the first time in a cluster (see Renzini and Buzzoni 1986 for a detailed discussion of this point). The reddening in the colour prior to the onset of the AGB phase is caused by those stars more massive than M_{up} that spent an appreciable fraction of their lifetime, a few 10^5 years, along the Hayashi line in stages following central He-exhaustion and prior to core C-ignition in non degenerate conditions.

v) There is an age range (approximately from 3×10^8 to 1×10^9 years) in which clusters of very different metallicity possess the same $(B-V)_o$ colour.

6.2 Determining the Age of Clusters from their Integrated Photometry

In principle, despite the uncertainty generated by the stochastic nature of the IMF (see the discussion by Chiosi et al. 1988 on the subject), the colour-age relationships discussed in the previous section could be used to date clusters of various chemical composition when only the integrated colours are known. To this aim the colour-age relationships must be tested against clusters for which both colours and independent estimates of the age are available. While the integrated colours are obtained by direct observational measurements, ages can be derived from one of the following methods: i) Main Sequence turn-off and termination magnitudes. ii) The red giant star luminosity, and iii) The maximum AGB luminosity. Since all the details relative to the methods in question are given in Chiosi et al. (1988), they will not be repeated here. Using one of the above methods, ages have been derived for a sample of selected clusters (Chiosi et al. 1988). Although the chemical abundances used to derive the theoretical calibrations may not be fully suited to the clusters in question, the agreement between theory and observations is fairly good, thus confirming the validity of our calibrations. Better comparison will be possible only when accurate and homogeneous determinations of chemical abundances for individual clusters will be obtained, and the corresponding calibrating relationships calculated.

However, only a small number of clusters out of the sample for which integrated colours have been measured, possess all the information required to date them on the basis of colour magnitude diagrams (turn off and main sequence termination luminosities, red giant clump luminosity, brightest AGB stars luminosities). On the other hand, it may be worth of interest to rank clusters as a function of the age even in those (more numerous) cases, in which only

integrated colours and magnitudes are available. To this aim we follow the method proposed by Elson and Fall (1985), which from the location of any cluster in the (U-B) versus (B-V) plane enables us to assign the so-called parameter S, analogous to the SWB types, to all of them (see Elson and Fall 1985, for more details). With the aid of those clusters for which both age and S are known, we get the following relation

$$\text{Log } t = 0.062\ S + 6.99, \qquad (6)$$

where t is the age in years, and in turn a relation between SWB and S or t. Relations (6) is somewhat different from the correspondent one by Elson and Fall (1985). This arises only from the different ages assigned to the calibrating clusters in virtue of the novel isochrones from models with convective overshoot.

6.3 The Colour Gap: Phase Transition or Cluster Formation History ?

It has been known for long time that the integrated magnitude V versus (B-V) diagram of LMC (as well as SMC) clusters shows a gap in the colour range $0.4 < (B-V) < 0.6$, in the sense that very few clusters of any total luminosity fall in this region (van den Bergh 1981). A similar gap seems to occur also in the plane (B-V) versus cluster type (SWB) of Searle et al. (1980), the transition being centered at type IV. Several explanations have been advanced: age gap and/or effects of cluster disruption (van den Bergh 1981); RGB and/or AGB phase transitions, in that the sudden appearance of those phases would drastically redden the colour on a very short time scale (Gascoigne 1980; Renzini 1981; Renzini and Buzzoni 1983); transition of the core He-burning phase from loop to clump. All these possibilities have been recently discussed by Renzini and Buzzoni (1986). However, none of these has been yet quantitatively tested on the basis of detailed colour evolution models.

Although the preference goes to the RGB and/or AGB hypotheses, the calibrating relationships we have presented in so far show little evidence of this. In fact, although these phase transitions are included in the derivation of the integrated fluxes, there is no visible effect in the integrated $(B-V)_o$ and $(U-B)_o$ colours. We are therefore inclined to conclude that the colour gap originates from other causes, among which we recall the effect of a period of star formation inactivity in LMC, the result of the rapid disruption and/or fading of the young blue clusters as suggested by van den Bergh (1981), or the superposition of these two.

6.4 The Age Distribution of LMC Clusters

In order to test the hypothesis of periods of inactivity in the cluster formation history, we derive the age distribution function and check whether the observational data are consistent with the idea that the cluster formation proceeded in bursts of activity.

To this aim, we follow the study of Elson and Fall (1985), who derived the age distribution (dN/dt) for a mass limited sample of LMC clusters sorted out from the van den Bergh (1981) list. The cluster mass is limited by means of theoretical fading lines in the B versus S plane. The fading line is locus along which a cluster of given total number of stars hence mass would evolve at increasing age. The number of clusters falling in each S or age bin is then corrected for photometric completeness. Adapting Elson's and Fall' (1985) precedure to the ages we are using, we get the following relation

$$\Delta N/\Delta t = 2.39\ 10^{-7}\ \Delta N' \ /\ (\ 10^{0.062\ S}) \ . \qquad (7)$$

The resulting age distribution (dN/dt) is shown in Fig.8 and compared to that by Elson and Fall (1985). The different slope of the two age distributions arises from the different S(t) relation. There are several glitches in the present age distribution which do not occur in that one by Elson and Fall (1985). In principle they could be attributed to discontinuities in the history of cluster formation. However, on one hand no great statistical significance can be given to those glitches owing to the large error bars (the square root of N), on the other hand it goes without saying that the age distribution is somewhat dependent on the adopted age binning. On the basis of the above considerations and in agreement to what already pointed out by Elson and Fall (1985), it seems reasonable to conclude that there is no convincing evidence for strong discontinuities in the rate of formation of LMC clusters, even though they cannot be definitely ruled out.

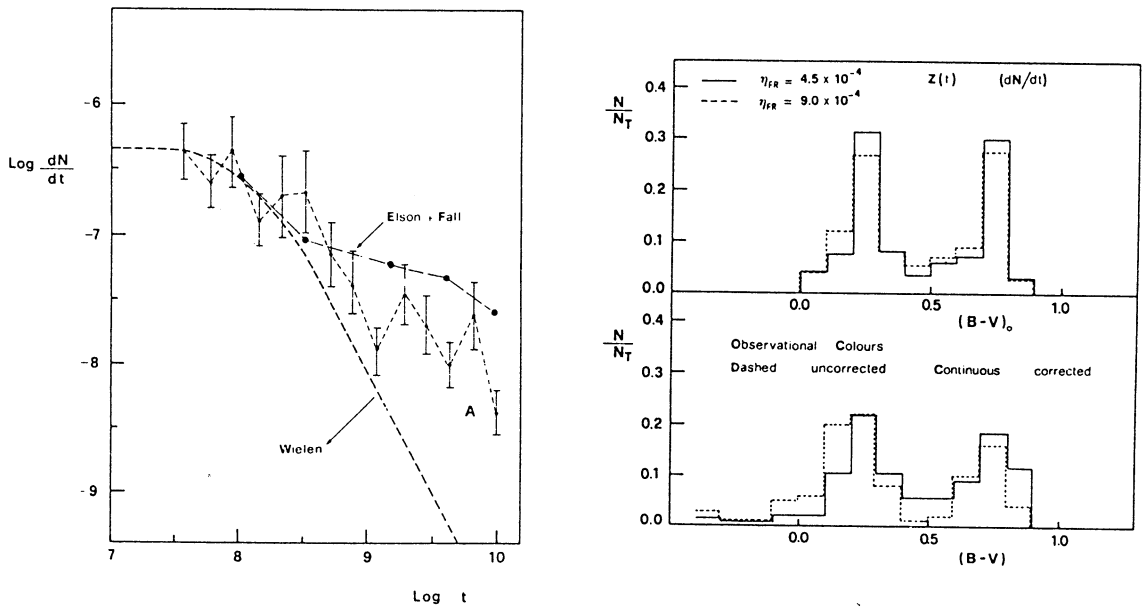

Fig.8 Age distribution for the mass limited sample of LMC clusters from the Chiosi et al (1988) (thin dashed line labelled A) and Elson and Fall (19985) (full circles). The vertical bars give an idea of the uncertainty in counting the number of clusters per age bin. The heavy dashed line shows the data for galactic open clusters determined by Wielen (1971). All (dN/dt)'s are in arbitrary units and normalized at the blue side

Fig.9 The colour distribution. The bottom panel shows the observational data before and after correction for photometric incompleteness. The top panel displays the theoretical distribution expected from eq. (8) when the observational (dN/dt), the colour-age relations with the Fusi-Pecci and Renzini (1976) mass loss rate as indicated by η_{FR}, and a linera dependence for the law of metal enrichment are adopted (see the text for more details)

6.5 The Colour Distribution of LMC Clusters

As already recalled, the number frequency distribution of (B-V) colours of LMC clusters is bimodal with two peaks centered at about 0.1 and 0.6 and a gap ranging from 0.2 to 0.5. The bottom panel (a) of Fig.9 shows the frequency histogram (number N of clusters per colour bin normalized to the total number N_T) obtained sampling the data of van den Bergh (1981) and Mateo and Hodge (1987) for 164 clusters in total. Before comparing the observational distributions of colours with the theoretical ones we agre going to derive, the former must be corrected for photometrical incompleteness similarly to what has been done for the age distribution function. Since per each age range we know the number of clusters added to the observational one to account for incompletenesss. the same number has been added to the number of clusters in each colour range. The conversion from age to colour is possible with the aid of the age versus S relation and the diagram (U-B) versus (B-V), which correlates S to colours. After correction, the total number of clusters increases to 307 and the colour distribution (bottom panel of Fig.9) is somewhat different from the previous one. The theoretical colour distribution distribution function f[(B-V)o] is

$$f[(B-V)o] = (dN/dt) \; / \; (d(B-V)_o/dt) \qquad (8)$$

where (dN/dt) is the observational age distribution function and $d(B-V)_o/dt$ is the colour speed. This latter can be easily derived from any colour-age relationship. To refine our colour speed, we also consider the possibility that some degree of metal enrichment over the galaxian lifetime is required to fully match the data. Such an hypothesis is certainly not ad hoc, as many arguments exist in literature supporting this fact (see Chiosi and Matteucci 1983; Cohen 1982; Hartwick and Cowley 1981; Searle and Smith 1981). To test this point in a simple manner,

we derived integrated colours $(B-V)_o$ and $(U-B)_o$ supposing that the cluster stellar population has increased its metal content with time. A linear relation has been assumed, assuming Z to be zero $15x10^9$ years ago and equal to 0.02 at the present epoch. This would suitable modify the (B-V)o versus age relation. This is shown in Fig.10 together with the observational data. These are the cluster of van den Bergh (1981) and Mateo and Hodge (1987). Superposition of the theoretical calibration to the observational data has been made assuming a mean $E_{B-V} = 0.10$. In the same figure we also show the relations S(t), S(SBW) and SWB(t). Although various causes, such as dispersion in the metal content and reddening, stochastic effects in the colours caused by the finite number of stars in a cluster, uncertainties in the age assignment to individual clusters, together with uncertainties in the theoretical calibrations may concur to scatter the data in the diagram of Fig.10, still the agreement between theory and observations is now remarkably good. The accompanying colour distribution functions are given in the top panel of Fig.9, together with the the observational ones (panel a) for comparison. This have been claculated assuming the mass loss rate by Fusi-Pecci and Renzini (1976) with their parameter η_{FR}. The effect of varying the algorithm for the mass loss rate is marginal. The careful analysis of the dependence of the colour distribution on the various factors contributing to it clarifies that it is primarily reflective of the age distribution, which determines the ratio of the blue to red clusters, whereas the colour speed fixes the location and width of the gap. In, particular we point out that the colour gap cannot be simply attributed to the increase in the mean metallicity of the gas with galaxian age (Frenk and Fall 1982). In fact, even including the increase in metallicity, the right colour distribution is obtained only with the observational age distribution.

6.6 Determining the Mass of Clusters from their Integrated Photometry

In principle it is possible to get information on the mass of a cluster out of its integrated magnitudes and colours. With the aid of eq.(1) and eq. (2) together with a suitable expression for the mass of stars in the cluster as function of the age. The procedure works as follows. The normalization constant A is given by

$$\log A = 0.4\ (M_{\Delta\lambda t} - M_{\Delta\lambda o} + DM + A_{\Delta\lambda}) \qquad (9)$$

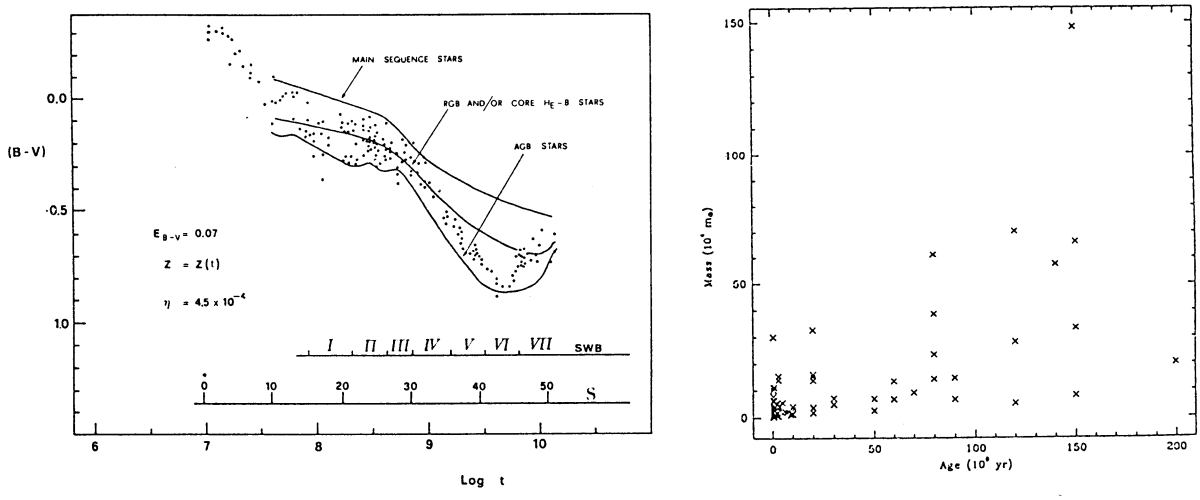

Fig.10 The (B-V) versus age relation, separated in its three main components, for a population of clusters whose mean metallicity is supposed to increase with the galaxy age. The particular case shown here refers to the mass loss rate of Fusi-Pecci and Renzini with $\eta_{FR} = 4.5x10^{-4}$. The mean colour excess $E_{B-V} = 0.07$ has been assumed to trnsfer theoretical colours into the observational ones. The relations between the parametrer S and age and the Searle et al (1980) type (SWB) and age are shown on separate scales. Ages are in years

Fig.11 Total masses of clusters in LMC from the van den Bergh (1981) sample calculated from their integrated V magnitudes as a function of the age obtained from their integrated (B-V) clours. Masses are in units of 10^4 $M_\odot$, whereas ages are in units of 10^8 yr

where $M_{\Delta\lambda t}$ and $M_{\Delta\lambda o}$ are the theoretical and observed integrated magnitudes in a given passband (V for instance), DM is the distance modulus and $A_{\Delta\lambda}$ is the reddening in that passband. Furtheremore, the total mass of stars in the cluster can be expressed as

$$M_{tot} = A\int_{M_L}^{M_U(t)} M\,\Phi(M)\,dM + A\int_{M_U(t)}^{M_U} M_x(M)\,\Phi(M)\,dM \qquad (10)$$

where $M_U(t)$ is the maximum mass of living stars in the cluster at that particular age, whereas M_x is the mass of remnants. M_U and M_L have been already defined in section 2. Having an estimate of the age and metallicity, we may infer $M_{\Delta\lambda t}$ from theory, fix the normalization constant A, and finally determine the mass of the cluster. It goes without saying that this will depend on the slope of the initial mass function and the assumed lower limit M_L for main sequence stars. The results obtained by Alongi and Chiosi (1989) assuming x = 1.35 M_L = 0.05 $M_\odot$ and M_U = 100 $M_\odot$ are shown in Fig.11 for the clusters with known A_V and M_{Vo}.

7. Star Formation in the Fields of LMC

A recent study of stellar fields in LMC by Mateo et al. (1989) has shown that the distribution of stars in the C-M diagrams V versus (B-V) is compatible with a law of star formation schematically approximated by a long period of lower efficiency followed by a global enhancement that began about 3 to 4 Gyr ago. The ratio of the past to recent level of star formation, called the enhancement factor α, that yield a good agreement between theoretical simulations and observational C-M diagrams, is about 5. Other time dependences for the law of star formation would not reproduce the relative percentages of stars in different areas of the C-M diagram. The details of this study can be found in Mateo et al. (1989).

Acknowledgements

This work has been financially supported by the Ministry of Public Education (Funds 40% and 60% MPI), and the Italian Space Agency (ASI). I like to express my deepest gratitude to Silvia Torres-Peimbert, Louis Carrasco, Alfonso Serrano, Manuel Peimbert and all the colleagues of the Department of Astronomy of UNAM for the warm hospitality. Finally I want to thank the financial support from UNAM that allowed me to attend this enjoable meeting.

References

Alongi, M., Chiosi, C. (1989). Preprint
Arimoto, N., Yoshii, Y. (1986). Astron. Astrophys. 164, 260
Baird, S., Flower, P., Hodge, P., Szkody, P. (1974). Astron. J. 79, 1365
Bathia, R.K., Hatzidimitriou, D. (1988). Mon. Not. Roy. Astr.Soc. 230, 215
Bathia, R.K., Hatzidimitriou, D. Cannon, R.D. (1989). Preprint
Bathia, R.K., MacGillivray, H.T. (1988). Astron. Astrophys. 203, L5
Barbaro, G. (1981). Astrophys. Sp. Sci. 77, 23
Barbaro, G. (1982). Astrophys. Sp. Sci. 83, 143
Barbaro, G., Bertelli, G. (1977). Astron. Astrophys. 54, 243
Barbaro, G., Pigatto, L. (1984). Astron Astrophys. 136, 355
Becker, S.A. (1981). Astrophys. J. Suppl. 45, 478
Becker, S. A., Iben, I. Jr. (1979). Astrophys. J. 232, 831
Becker, S. A., Mathews, G. J. (1983). Astrophys. J. 270, 155
Bell, R. A., Gustafsson, B. (1978). Astron. Astrophys. Suppl. 34, 229
van den Bergh, S. (1981). Astron. Astrophys. Suppl. 46, 79
Bertelli, G., Bressan, A., Chiosi, C. (1985). Astron. Astrophys. 150, 33
Bertelli, G., Bressan, A., Chiosi, C., Angerer, K. (1986a). Astron. Astrophys. Suppl. Ser. 66, 191
Bertelli, G., Bressan, A., Chiosi, C., Angerer, K. (1986b). In "The Age of Star Clusters", ed. F. Caputo, Mem. Soc. Astron. It. 57, 427
Boothroyd, A. I., Sackmann, I. J. (1988a). Astrophys. J. 328, 632
Boothroyd, A. I., Sackmann, I. J. (1988b). Astrophys. J. 328, 641
Boothroyd, A. I., Sackmann, I. J. (1988c). Astrophys. J. 328, 653
Boothroyd, A. I., Sackmann, I. J. (1988d). Astrophys. J. 328, 671

Bressan, A., Bertelli, G., Chiosi, C. (1981). Astron. Astrophys. 102, 25
Bressan, A., Bertelli, G., Chiosi, C. (1986). In "The Age of Star Clusters", ed. F. Caputo. Mem. Soc. Astron. It. 57, 411
Bruzual, A. G. (1983). Astrophys. J. 273, 105
Buonanno, R., Corsi, C. E., Fusi-Pecci, F. (1985). Astron. Astrophys. 145, 97
Burstein, D. Heiles, C. (1982). Astron. J. 87, 1165
Buser, R., Kurucz, R. L. (1978). Astron. Astrophys. 70, 555
Castellani, V., Chieffi, A., Pulone, L., Tornambe', A. (1985). Astrophys. J. 296, 204
Chieffi, A., Straniero, O. (1988). Astron. Astrophys. Submitted
Chiosi, C. (1986). In "Nucleosynthesis and Stellar Evolution", 16th Saas-Fee Course, ed. B. Hauck et al., p. 199, Geneva Observatory
Chiosi, C., Bertelli, G., Bressan, A. (1987). In "Late Stages of Stellar Evolution", ed. S. Kwok and S. R. Pottasch, p. 239, Dordrecht: Reidel
Chiosi, C., Bertelli, G., Bressan, A. (1988). Astron. Astrophys. 196, 84
Chiosi, C., Bertelli, G., Meylan, G., Ortolani, S. (1989a). Astron. Astrophys. Suppl. in press
Chiosi, C., Bertelli, G., Meylan, G., Ortolani, S. (1989b). Astron. Astrophys. in press
Chiosi, C., Maeder, A. (1986). Ann. Rev. Astron. Astrophys. 24, 329
Chiosi, C., Matteucci, F. (1983). Astron. Astrophys. 105, 140
Cohen, J. G. (1982). Astrophys. J. 258, 143
Da Costa, G. S., Mould, J., Crawford, M. D. (1984). Astrophys. J. 280, 595
Eggen, O.J., Iben, I.Jr. (1988). Astron. J. 96, 635
Eggen, O.J., Iben, I.Jr. (1989). Astron. J. 97, 431
Elmegreen, B.G., Elmegreen, D.M. (1983). Mont. Not. Roy. Astr. Soc.203, 31
Elson, R. A. W., Fall S. M. (1985). Astrophys. J. 299, 211
Elson, R.A.W., Fall, S.M., Freeman, K.C. (1987). Astrophys. J. 323, 54
Elson, R.A.W., Fall, S.M., Freeman, K.C. (1989). Astrophys. J. 336, 734
Frenk, C.S., Fall, S.M. (1982). Mon. Not. R. Astr. Soc. 199, 565
Fusi-Pecci, F., Renzini, A. (1976). Astron. Astrophys. 46, 447
Gascoigne, S. C. B. (1980). In "Star Clusters", ed. J. Hesser, p. 305. Dordrecht: Reidel
Green, E. M., Demarque P., King, C. R. (1987). "The Revised Yale Isochrones and Luminosity Functions (Yale University, Observatory, New Haven
Gustafsson, B., Bell, R. A., Eriksson, K., Nordlund, A. (1975). Astron. Astrophys. 42, 407
Hartwick F. D. A., Cowley, A. (1981). In "Astrophysical Parameters for Globular Clusters" eds. A. G. D. Philip & D. S. Hayes, L. Davis Press Inc., New York, p. 205
Heckman, T. M. (1976). Astrophys. J. Suppl. 36, 451
Hodge, P.W. (1963). Astrophys. J. 137, 1033
Hodge, P.W. (1984). Pub. Astron. Soc. Pacific 96, 947
Hollowell, D. E. (1987). in "Late Stages of Stellar Evolution", ed. S. Kwok and S. R. Pottasch, p. 239, Dordrecht: Reidel
Hollowell, D. E. (1988). Ph. D. Thesis, University of Illinois
Iben, I. Jr. (1975a). Astrophys. J. 196, 525
Iben, I. Jr. (1975b). Astrophys. J. 196, 549
Iben, I. Jr. (1976). Astrophys. J. 208, 165
Iben, I.Jr., Renzini, A. (1983). Ann. Rev. Astron. Astrophys. 21, 271
Larson, R.B. (1989). In "Structure and Dynamics of the Interstellar Medium", IAU Colloquium n. 120, eds. M. Moles, G. Tenorio Tagle and J. Melnick (Berlin, Springer-Verlag), in press
Lattanzio, J. C. (1986). Astrophys. J. 311, 708
Lattanzio, J. C. (1987a). In "Late Stages of Stellar Evolution", ed. S. Kwok and S. R. Pottasch, p. 235, Dordrecht: Reidel
Lattanzio, J. C. (1987b). Astrophys. J. Lett. 313, L15
Lattanzio, J. C. (1988a). In "Evolution of Peculiar Red Giant Stars", In press
Lattanzio, J. C. (1988b). In "Origin and Distribution of the Elements", ed. G. J. Mathews, p. 398, Singapore: World Scientific
Lattanzio, J.C. (1989). UCRL-100238 preprint
Maeder, A. (1974). Astron. Astrophys. 32, 177
Maeder, A., Meynet, G. (1989). Astron. Astrophys. 210, 155
Manteiga, M., Pickles, A.J., Martinez Roger, C. (1989). Astron. Astrophys. 210, 66
Mateo, M. (1988). Astrophys. J. 331, 261
Mateo, M., Chiosi, C., Bertelli, G. (1989). Preprint
Mateo, M., Hodge, P. (1986a). Astrophys. J. 311, 113
Mateo, M., Hodge, P. (1986b). Astrophys. J. Suppl. 60, 893
Mateo, M., Hodge, P. (1987). Astrophys. J. 320,626

Mateo, M., Hodge P. W. (1987). Private Communication
Mazzitelli, I., D'Antona, F. (1986). Astrophys. J. 311, 762
McCrea, W.H. (1964). Mon. Not. R. Astron. Soc. 128, 147
Meylan, G. (1987a). Astron. Astrophys. 184, 144
Meylan, G. (1987b). In "Stellar Evolution and Dynamics in the Outer Halo of the Galaxy, eds. M. Azzopardi, F. Matteucci, Garching, ESO, p. 665
Meylan, G. (1988). Astron. Astrophys. 191, 215
Meylan, G., Djorgovski, S. (1987). Astrophys. J. Lett. 322, L94
Persson, S. E., Aaronson, M., Cohen, J. G., Frogel, J. A., Matthews, K. (1983). Astrophys. J. 266, 105
Rabin, D. (1982). Astrophys. J. 261, 85
Reimers, D. (1975). Mem. Soc. Roy. Sci. Liege 6 serie, tome 8,p. 369
Renzini, A. (1981). Ann. Phys. Fr. 6, 87
Renzini, A., Buzzoni, A. (1983). Mem. Soc. Astron. It. 54, 739
Renzini, A., Buzzoni, A. (1986). In "Spectral Evolution of Galaxies", ed. C. Chiosi, A. Renzini, p. 195. Dordrecht: Reidel
Renzini, A., Voli, M. (1981). Astron. Astrophys. 94, 175
Salpeter, E. E. (1955). Astrophys. J. 121, 161
Searle, L., Sargent, W. L. W., Bagnuolo, W. G. (1973). Astrophys. J. 179, 427
Searle, L., Smith, H. (1981). In "Astrophysical Parameters for Globular Clusters", eds. A. G. D. Philip and D. S. Hayes, L. Davis Press Inc., New York, p. 201
Searle, L., Wilkinson, A., Bagnuolo, W. G. (1980). Astrophys. J. 239, 803
Storm, J., Andersen, J., Blecha, A., Walker, M. F. (1988). Astron. Astrophys. 190, L18
Vallenari, A., Chiosi, C., Bertelli, G., Meylan, G., Ortolani, S. (1989). Astron. J. submitted
Walker, A. R. (1987). Mon. Not. R. Astr. Soc. 225, 627
Welch, D. L., McLaren, R. A., Madore, B. F., McAlary, C. W. (1987). Astrophys.J. 321, 162
Wielen, R. (1971). Astron. Astrophys. 13, 309

Cesare Chiosi: Departamento di Astronomia, Universitá di Padova, I-35100 Padova, Italy.